Naturwissenschaften (2014) 101:87–94
DOI 10.1007/s00114-013-1133-3

ORIGINAL PAPER

Shifting wavelengths of ultraweak photon emissions from dying melanoma cells: their chemical enhancement and blocking are predicted by Cosic's theory of resonant recognition model for macromolecules

Blake T. Dotta · Nirosha J. Murugan · Lukasz M. Karbowski · Robert M. Lafrenie · Michael A. Persinger

Received: 27 September 2013 / Revised: 15 December 2013 / Accepted: 17 December 2013 / Published online: 15 January 2014

Abstract During the first 24 h after removal from incubation, melanoma cells in culture displayed reliable increases in emissions of photons of specific wavelengths during discrete portions of this interval. Applications of specific filters revealed marked and protracted increases in infrared (950 nm) photons about 7 h after removal followed 3 h later by marked and protracted increases in near ultraviolet (370 nm) photon emissions. Specific wavelengths within the visible (400 to 800 nm) peaked 12 to 24 h later. Specific activators or inhibitors for specific wavelengths based upon Cosic's resonant recognition model elicited either enhancement or diminishment of photons at the specific wavelength as predicted. Inhibitors or activators predicted for other wavelengths, even within 10 nm, were less or not effective. There is now evidence for quantitative coupling between the wavelength of photon emissions and intrinsic cellular chemistry. The results are consistent with initial activation of signaling molecules associated with infrared followed about 3 h later by growth and protein-structural factors associated with ultraviolet. The greater-than-expected photon counts compared with raw measures through the various filters, which also function as reflective material to other photons, suggest that photons of different wavelengths might be self-stimulatory and could play a significant role in cell-to-cell communication.

Keywords Photon emissions · Cosic resonant recognition model · Melanoma cells · Near infrared · Near ultraviolet

Communicated by: Sven Thatje

B. T. Dotta · N. J. Murugan · L. M. Karbowski · R. M. Lafrenie · M. A. Persinger (✉)
Biomolecular Sciences Program, Laurentian University, 935 Ramsey Lake Road, Sudbury, Ontario, Canada P3E 2C6
e-mail: mpersinger@laurentian.ca

Introduction

Ultraweak photon emissions (UPE) have been measured from cells, organs, and organisms (Chang and Popp 1998), but the precise coupling between molecular pathways and specific wavelengths of these pervasive electromagnetic phenomena have not been completely established. Popp (1988) has argued that all living tissue display very weak photon emissions. Several decades ago Gurwitsch (1923) suggested that "mitogenetic radiation" or photons within biological tissue could trigger and regulate cell growth. Biophotons have recently been demonstrated by in situ biophoton autography to behave as neural communication signals (Sun et al. 2010). The numbers of photons emitted are in the order of a few to a few hundred per second per square centimeter and require measurement by photomultiplier tubes.

The quanta of energies associated with the photons vary depending upon the state of the cells and can range from the ultraviolet through the visible range into the infrared. Cohen and Popp (1997) indicate that the emissions continuously cover the spectral range from at least 200 to 800 nm. Tilbury and Quickenden (1988), employing cultures of *Escherichia coli*, found that the ultraviolet (210–300 nm) and visible (450–620 nm) regions were associated with the exponential phase of growth while a second period or stationary phase of growth produced photons only in the visible region. The magnitude of these emissions was in the order of 10^3 counts s^{-1}.

That applied light of specific frequencies affect cell growth has received recent attention. Wu and Persinger (2011) reported increased stem cell proliferation in sectioned planarian following exposure to 880-nm light-emitting diodes (LED) compared with incandescent red or white light or darkness and ambient light; a similar effect with 685-nm laser radiation was found by de Souza et al. (2005). Treatment of primary rat

cortical neurons, following ischemia, by 710-nm light promoted synaptogenesis through MAPK activation (Choi et al. 2012). Photobiomodulation, depending upon wavelength, can stimulate or inhibit biological functions without producing irreducible damage (Liu et al. 2009). In fact, shrinkage of tumors occurs after exposure to near-infrared light in target cells that express the receptor for epidermal growth factor (Mitsunaga et al. 2011).

Although original research utilized paradigms where luminescence was measured in cells following irradiation of light with varying wavelengths, the occurrence of "degradation radiation" (Popp 1979) from dying cells has been considered a means by which one could study the nature of the cellular states. Dotta et al. (2011a) measured photon flux density from eight different cell lines for 24 h after removal from incubation. One of the types, B16–BL6 (mouse melanoma) cells, demonstrated a conspicuous emission profile. Exposure of ~10^6 of these cells to compounds related to signaling pathways and synchronized M- and S-phase measures strongly suggested that the plasma cell membrane was the source of the UPE and that the rates were in the order of 10^{-20} J s^{-1} $cell^{-1}$ (Dotta et al. 2011a). The photon flux density was ~10^{-11} W m^{-2} for ~1 million cells which was comparable to levels found in other tissue from other studies (Isojima et al. 1995).

In the present experiments, we decided to discern if the wavelengths of the photon emissions changed over the first 24 h after the cells had been removed from incubation. Pilot studies had indicated powerful and reliable emissions at specific wavelengths. In order to couple the specific wavelengths with the molecular activity within the cell, we required a rational mechanism by which specific molecular compounds could be selected. In 1994, Cosic (1994) published a new physicomathematical approach, the Resonant Recognition Model (RRM). It was based upon the representation of the protein primary structure as a numerical series. This was accomplished by assigning each amino acid a physical value (specifically the energy of delocalized electrons for each amino acid) that was relevant to the protein's biological activity. She obtained characteristic RRM frequencies for different functional groups of proteins and DNA regulatory sequences.

Cosic had developed this model to explain the unexpected but significant resemblances between functionally dissimilar proteins and the nonsignificant similarities between functionally related peptides. Previously, we (Wu and Persinger 2011) found that the wavelength predicted from Cosic's procedure for cyctochrome *c* and cytochrome oxidase II (proteins most likely involved with regenerating planarian blastema) was within error range of our effective infrared treatment. Here, we present evidence that photons with different wavelengths display different peak activities as melanoma cells respond to the change from incubators to ambient temperature and that these specific emissions can be blocked or facilitated by promoters or inhibitors predicted by the Cosic model.

Methods

Over several months a total of 60 experiments were completed on separate days. For each experiment, approximately one million B16 cells approaching 100 % confluence were used for measurement. Cells were maintained in 150×20 mm tissue culture plates (Sarstedt, Laval, Qc) in Dulbecco's modified essential medium (DMEM; Hyclone, Logan, UT) supplemented with 10 % fetal bovine serum, 100 μg/m streptomycin, and 100 U/mL penicillin (Invitrogen, Burlington, ON). Cells were incubated at 37 °C in 5 % CO_2 and subcultured 1:5 about every 4 days. The cell monolayers were washed with PBS, pH 7.4 and harvested by incubation in 0.25 % trypsin-EDTA and then collected by centrifugation at 1,000×g for 10 min. All treatments were added to cell culture plates ~30–60 min prior to photon emission measurement. After removal from the incubator the single plate of ~10^6 cells was transported to the biophysics area within 30–60 min and placed over the 3-cm^2 aperture of a SENS-TECH LTD. Model DM0090C digital photomultiplier tube (PMT). The rationale for removing the cells from physiological temperature was based on past research indicating that stressed cells produced consistent robust emission levels at ambient temperature (Dotta et al. 2011a). According to specifications, the range of sensitivity for photons was 280 to 850 nm. Typical dark counts of this PMT were in the range of 15–16 counts/s. Measurements were recorded by the system software every 2.5 s for 22.5 h (the maximum rate and duration determined by the software). Compared with dark counts, a plate of 10^6 cells generated about 40 to 55 counts s^{-1} above noise during the beginning of the experiment and about 5 to 10 counts s^{-1} above noise by the end of the experiment. In addition, controls were performed with a single plate with only medium and with no plate whatsoever. Both of these control conditions produced null results. While typical averaged absolute counts in the first hours averaged 35–40 counts s^{-1}, the first few minutes (5–15 min) consistently produced absolute values in the 80–120 counts s^{-1} range.

Assuming 5 10^{-19} J/photon for mid-range light, an average 55 photons s^{-1} and a cross section area of the aperture of ~3 10^{-4} m^2, the irradiance flux density would have been about 1.1 10^{-13} W m^{-2}. However, because the ~0.5 million cells were confluent over the 28-cm^2 of the dish but the aperture was only 3 cm^2 across, the UPE would have been measured from 0.11 of the total dish area (about 10^5 cells). The light generated in 3-D space by the single layer of cells in one direction to the aperture (πr^2) relative to the area of the sphere from the plane of the cells to PMT ($4\pi r^2$) about 1 cm in distance indicates that only about one fourth of the UPE would be recorded. Consequently, the effective flux density was ~0.4 10^{-11} W m^{-2} which is within the range of our previous measurements using a separate PMT model (Model 15 Photometer from Pacific Photometric Instruments with

photomultiplier tube housing for a RCA electron tube (BCA IP21)) (Dotta et al. 2011a).

All experimental conditions were completed in triplicate on different days. To discern the differential emissions from different wavelengths, the following bandpass filters (Chroma Technologies) were interposed between the PMT aperture and the bottom of the cell container: 370, 420, 490, 500, 620, 790, 950, and 995 nm. According to the manufacturer each filter selected the peak wavelength±5 nm. These filters are typically designed for normal incidence of the photon beam; however light emission from cells will be emitted at all angles. Consequently, it is possible that light approaching the filters at varying angles (i.e., 20°) exhibits wavelength shifts. To minimize this effect, cell dishes were placed directly over the filter (dish depth, 1 mm) and each condition involved multiple replicates to ensure the most accurate results.

These filters were selected based upon our theoretical approach (Cosic 1994) and to ensure coverage of the ultraviolet, visible, and infrared wavelength. In addition, we selected the 500- and 490-nm filters to investigate the functional "band width" of the effective light emissions for the biological functions. There was no response, i.e., a flat line activity of 15 photons s^{-1} for the 995-nm filter while the 950-nm showed marked cell-related activity. Given the various quantum efficiency values for each wavelength (~0.1 % for 995 nm and ~20 % for 420 nm), absolute photon counts for individual wavelengths may be higher than measured. Therefore, we focused on alterations of temporal profiles (enhancement/diminishment of peaks) rather than overall intensity.

Once the temporal profile for the peak photon emissions for the different wavelengths (the filters) were obtained, specific activators and inhibitors were selected based upon Cosic's calculation from:

$$\lambda = K/f_{\mathrm{RRM}}, \tag{1}$$

where λ is the wavelength of the light irradiation in nanometers, K is the RRM frequency space calculated by Cosic (1994), and f_{RRM} is the numerical frequency obtained by the RRM. The K value used was 201 with a standard deviation of 15 %. Here, λ was the wavelength of interest and K was Cosic's constant. After obtaining the f value, we consulted Cosic's tables for the protein family that optimally matched her f value (Cosic 1994).

For example, Cosic's value for 370 nm was 0.543, and because growth proteins (IGF) had been calculated with a value of 0.50, this class of proteins was used. For five different filters, we selected compounds from Cosic's table that were specific activators or inhibitors for the wavelength and those that were not specific activators or inhibitors, that is they were specific to another wavelength. We then obtained those compounds from what was available in our repertoire (Table 1).

The list of compounds and the specific filter were: 370 (inhibitor, Wortmannin), 420 (inhibitor, Genistein and activator, phorbol 12-myristate 13-acetate), 490 (inhibitor, 2-amino-6-chloro-α-cyano-3-(ethoxycarbonyl)-4H-1-benzopyran-4-acetic acid ethyl ester (SC79; activator, SQ22536), 500 (inhibitor, bisindolylmaleimide (BIS)), and 950 nm (inhibitor, PD (PD8059); activator, forskolin). These compounds were considered specific inhibitors or specific activators for that wavelength. The use of term nonspecific inhibitor or activator indicates the compound contained with the media for those cells whose UPE were measured was optimal for another filter. All chemicals were obtained from Sigma and from EMD Calbiochem. SQ22536 and Forskolin were prepared in DH_2O, all other were prepared in DMSO.

Given the range of the above wavelengths and the temporal differences in the appropriate directional responses to these compounds, we directly tested responses for the two most adjacent filters: 490 and 500 nm. When the 490-nm filter was employed, we tested the activator for 490 nm (SC79), the specific inhibitor for 490 (SQ), and the specific inhibitor for 500 nm (BIS), i.e., a nonspecific inhibitor. For 500 nm, we applied BIS (the specific inhibitor), SQ (the one most optimal for 490 nm, nonspecific inhibitor), and SC79 (the one most optimal for 490 nm as a specific activator).

The dilution was 1:1,000 and 2.5 μL of drug was added per 2.5 mL of media. All compounds were prepared at 10 μM concentrations except for BIS and SQ79 which were prepared at 5 μM concentrations. These concentrations were chosen based upon past research that elicited reliable increases in photon emissions from B16–BL6 mouse melanoma cells (Dotta et al. 2011a). The means of the absolute numbers of photons per sec for each treatment for each filter from the triplicates were analyzed as results. The baseline levels of photon counts s^{-1} for raw (no filters) when cells were not present were not significantly different from photon counts when cells were present with the 995-nm filter, suggesting that photon emissions from cells were <995 nm or that this threshold reflected the limits of the PMT. Where relevant, z-scores were calculated in order to compare UPE through different filters.

Results

The most conspicuous source of photon emissions from the melanoma cells during the first 24 h following removal from standard incubation was the marked increase in the numbers of UPE through the 370- and 950-nm filters. The results are shown in Fig. 1 and reflect the mean of three triplicates for each filter.

Table 1 List of individual wavelengths calculated *F*, potential protein target, and potential protein target's theoretical *F*

Wavelength (nm)	Calculated F ($f=K/\lambda$; K=201 SD 15 %)	Protein	Theoretical *F*
370	0.543	Insulin-like growth factors/ fibroblast growth factors	0.500/0.502
420	0.478	SOS operators, actin/myosin	0.468 and 0.488/0.340
490	0.410	Kinase-PI3K	0.429
500	0.402	Kinase-PKC	0.429
620	0.032	Lysosomes/glucagon	0.328/0.320
790	0.254	Growth factors/restriction enzymes	0.292/0.291
950	0.211	Signal proteins	0.214

Target protein's theoretical *F* is within ~0.15 of calculated *F*. These proteins were the specific targets of our inhibitors/activators

About 6 h after the removal from the incubators and after photon measurements began, there was a sudden increase in infrared (invisible) photons (950 nm) that were maintained for the remainder of the measurements. About 3.5 h after this increase, there was a second sudden increase in the ultraviolet (invisible) range (370 nm) that was also maintained for the remainder of the experiment. Lagging of the two curves by 3.5 h resulted in a correlation (Pearson's *r*) of ~0.85.

The second conspicuous effect is shown in Fig. 2 that includes the results for all of the filters including those within the visible wavelengths. In order to accommodate differences, the absolute values for the numbers of photons per second *z*-scores were obtained.

The interface between visible and infrared (790 nm) displayed a dramatic diminishment within an hour (~30 min) of removal from incubation. The major increases in photon emissions within the remainder of the visible range began after the 12th hour for the 620-, 500-, and 420-nm wavelengths. The 490-nm wavelength displayed a relative increase only at the end of the measurement period, at about 22 h. After the increase in photon emissions within the visible range, photons within the 950-nm range displayed a second peak emission. In comparison, the numbers of photons (about 10/s) through the 995 filter remained constant (flat line) across the entire experiment.

A clear relationship between wavelengths of photons associated with a particular filter and the class of compounds predicted by Cosic's equation was verified. As shown in Fig. 3, the photon counts through the 490-nm filter showed that specific activator (SQ22536) increased the photon counts while the specific inhibitor (SC79) diminished the photon counts by comparable numbers ($F(3, 31)=201.1$, $p=<0.001$, $eta^2=.95$).

Photon emissions after a nonspecific inhibitor (BIS) had been added to the cells did not differ from the values for untreated cells. The effects across the three triplicates completed on different days were consistent.

On the other hand, Fig. 4 demonstrates that when the two drugs that were selected specifically for the 490-nm Cosic

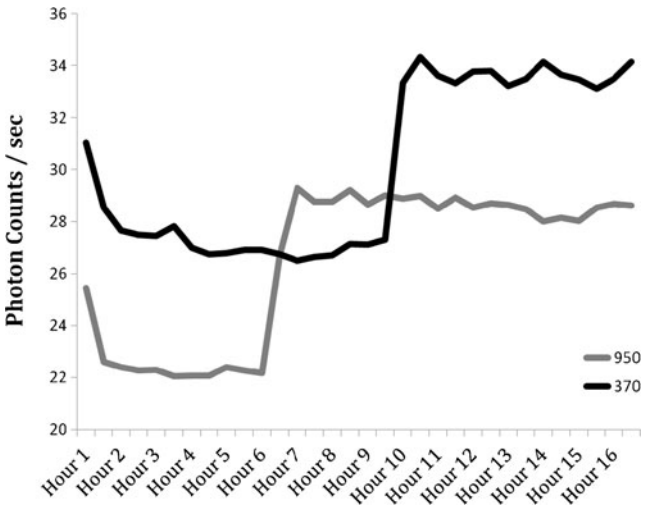

Fig. 1 Absolute photon counts (seconds) of two different filters (370 and 950 nm) as a function of time for untreated cell cultures (10^6 cells) removed from an incubator and placed at room temperature. *Black line* corresponds to 370 nm filter, whereas *grey line* corresponds to 950 nm filter

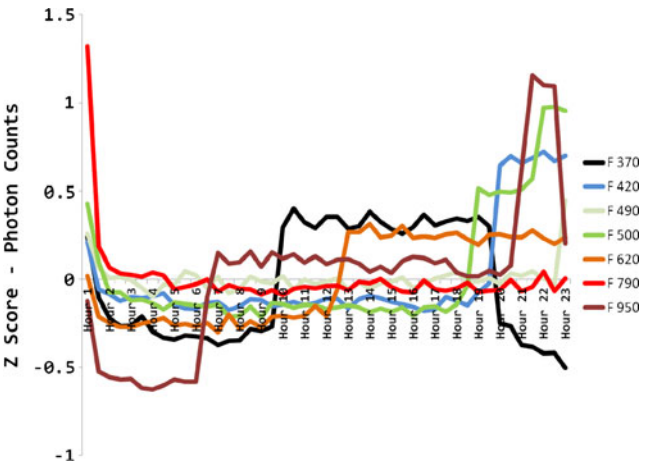

Fig. 2 Z-scored photon counts (seconds) for untreated cell cultures (10^6) removed from an incubator and placed at room temperature as a function of time. Each filter condition is in triplicate. The ranges of average absolute counts per second are: 370 (26–35 counts s^{-1}), 420 (22–30 counts s^{-1}), 490 (24–28 counts s^{-1}), 500 (23–35 counts s^{-1}), 620 (21–27 counts s^{-1}), 790 (22–30 counts s^{-1}), and 950 nm (22–37 counts s^{-1})

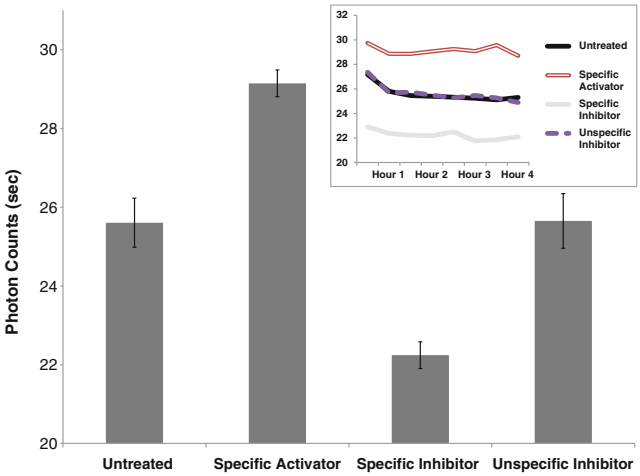

Fig. 3 Means and standard deviations of absolute photon counts per second for four separate treatment conditions of filter 490 during the first 4 h of testing. Untreated corresponds to the no-drug 490-nm condition; specific activator refers to SC79; specific inhibitor refers to SQ; and unspecific inhibitor refers to BIS. Raw data of each condition throughout the first 4 h can be seen in the upper right quadrant

solution were applied to cells when 500 nm photons were measured, there was no evidence of either persistent facilitation or inhibition of raw numbers of photon emissions. Only the specific inhibitor for the 500-nm filter photons produced significant inhibition of counts as demonstrated by one-way analysis of variance ($F(3, 179)=28.5$, $p=<0.001$, $eta^2=.32$]. What occurred was the shift when the maximum numbers of photons were emitted during the experiment. The specific inhibitor selected by Cosic criteria for the 500-nm wavelength (BIS) suppressed the photon emissions in this band throughout the experiment, whereas the nonspecific inhibitor (SC79)

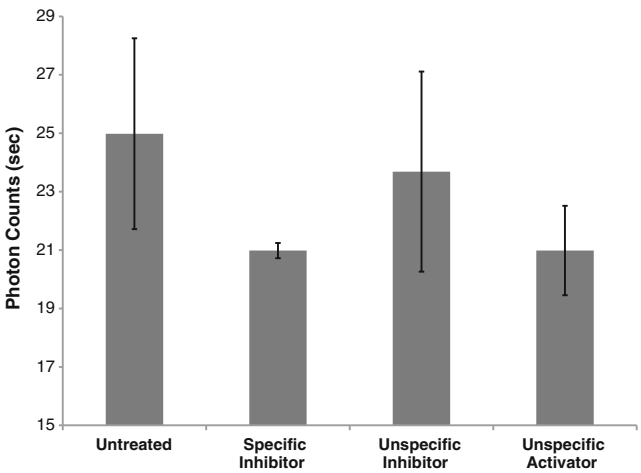

Fig. 4 Means and standard deviations of absolute photon counts per second for four separate treatment conditions of filter 500 during the entire testing sample (22.5 h). Untreated corresponds to the no-drug 500-nm condition; specific inhibitor refers to BIS, whereas unspecific inhibitor refers to SQ, and unspecific activator refers to SC79

diminished the emissions only between the 7th and 19th hours (Fig. 5). During the first few hours, it actually enhanced UPE.

Even the wavelengths associated with the largest numbers of photon emissions were inhibited by the appropriate Cosic-predicted molecules. As can be seen in Fig. 6, the inhibitor (PD8059) for 950 nm suppressed the powerful and protracted emission of photons from 6 h to the end of the experiment ($F(2, 32)=5.065$, $p=0.01$, $eta^2=.25$). The activator (forskolin) transiently increased emissions for the first 6 h. Following this transient elevation, there was a decrease in photon counts to baseline levels.

At the other end of the spectrum, 370 nm, the inhibitor (Wortmannin) based on this wavelength suppressed the increase in photon emissions during the period of 9 to 16 h but was no longer effective when enhancement began to drop after about 19 h. This can be seen in Fig. 7 ($F(1, 89)=151.2$, $p=>0.001$, $eta^2=.63$]. Wortmannin exhibits a very short half-life (~10 min). By hour 9, there would have been less than 1 mol./mL. However, we cannot discern when this effect, which ultimately produced the inhibition of UPE, actually occurred during that interval.

For the 500-nm filter, the specific inhibitor (BIS) flattened the UPE emission while the nonspecific inhibitor (SQ) and nonspecific activator (SC79) produced transient activation and inhibition of UPE.

In order to discern if the quantity of photons measured from specific filters for a given wavelength (±5 nm) were congruent with the total number of photons measured from these cells without filters, the percentages from each wavelength contributing to the overall photon counts were calculated. These results are shown in Fig. 8. The composition from the two nonvisible (370 nm and 950 nm) filters were equal to the combined output of the five visible wavelength filters. During the first 90 min, the combination for all seven (995 nm remained as a flat line) responsive filters (sum=60 nm) contributed to 30 to 40 % of the total photon output. The increasing trend noted in Fig. 8 continued until the end of the experiment.

Discussion

The results of these experiments demonstrated reliable and conspicuous shifts in specific bands of wavelengths of photon emissions from melanoma cells during the first 24 h following removal from incubation. By far the most obvious protracted effects were the relative increase in UPE through the infrared 950-nm filter after about 7 h followed about 3 h later by the marked enhancement of 370 nm photons. According to Cosic's theory to predict macromolecular bioactivity, the 950-nm band is associated with molecules involved with signaling activities within the cell as well as cell proliferation. The 370-nm band is more related to macromolecules involved with cell growth and structure. The discrepancy of about 3 h is very similar to the

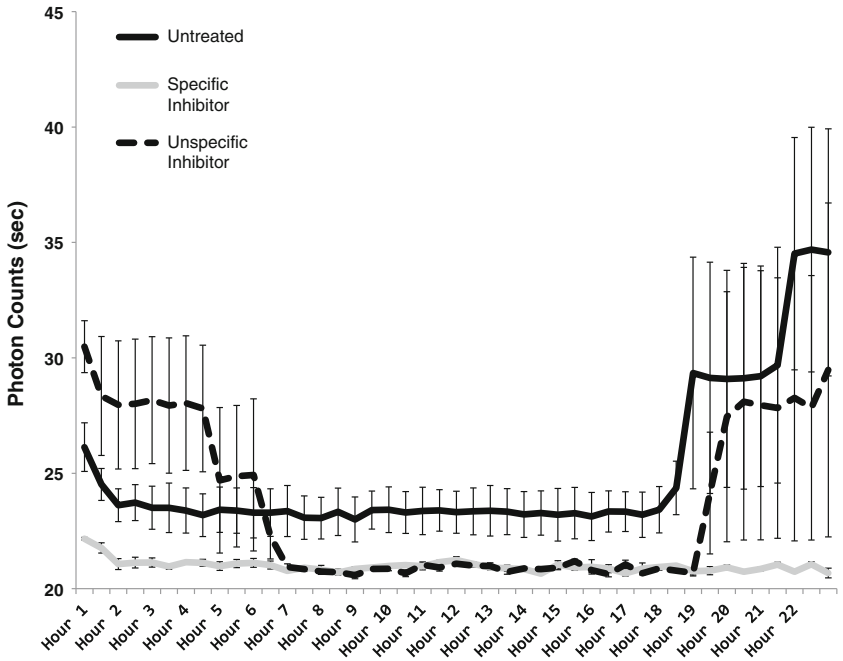

Fig. 5 Means and standard errors of absolute photon counts per second for three separate treatment conditions of filter 500 during the entire testing sample (22.5 h). Untreated corresponds to the no-drug 500-nm condition; specific inhibitor refers to BIS, and unspecific inhibitor refers to SQ

latency between cell signaling and the transcriptions of proteins (Gossen et al. 1994; Bensaude 2011; Bondos and Tan 2011).

The hypothesis that there are specific relationships between the numbers of photons emitted during Popp's "degradation radiation" within a specific wavelength and the corresponding molecular machinery was supported. When a specific activator predicted by Cosic' theory had been added to the media containing the cells during measurement of photons when the 490-nm filter was applied, the photon counts increased for several hours. When the specific inhibitor was added, there was a comparable magnitude of decrease in photon counts for several hours. The photon counts after a nonspecific inhibitor, which was considered more optimal for 500-nm wavelengths, had been added did not differ significantly from the untreated controls.

Conversely, when the inhibitor most optimal for the 500 nm was added to the media and the photon counts were

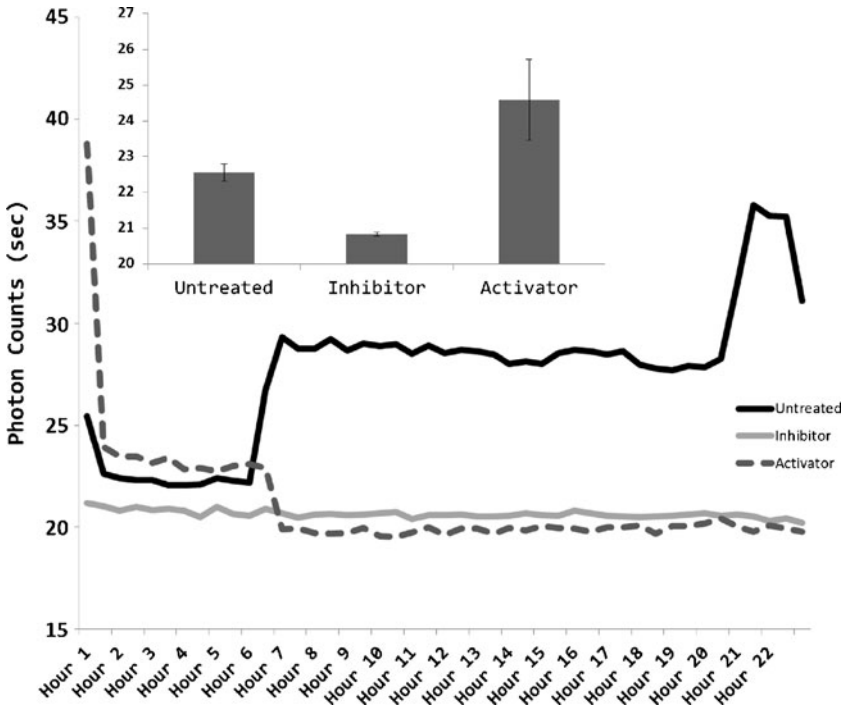

Fig. 6 Means of absolute photon counts (seconds) of Filter 950 with three separate treatment conditions as a function of time. Untreated refers to the no-drug 950-nm condition, inhibitor refers to PD, and activator refers to Forskolin. Means and standard error values for photon counts per second for the first 6 h of testing can be seen in the upper left quadrant

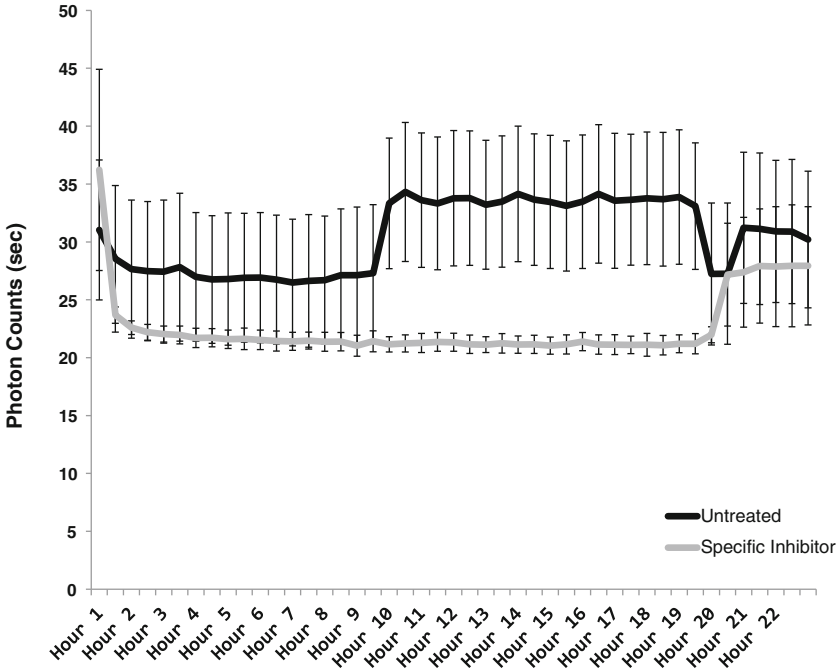

Fig. 7 Means and standard errors of absolute photon counts per second for two separate treatment conditions of filter 370 during the entire testing sample (22.5 h). Untreated corresponds to the no-drug 370-nm condition, inhibitor refers to Wortmannin

obtained through the 500-nm filter, there was persistent diminishment of emission. The nonspecific inhibitor (the optimal one for 490 nm) actually produced increased photons during the first 5 h, the opposite than what would be expected for an inhibitor, before diminishment was occurred. For narrow-band specificity, such as the molecular structure most optimally matched for sequestering to receptors, very small changes in morphology in a ligand can produce effects opposite to that of the traditional agonist.

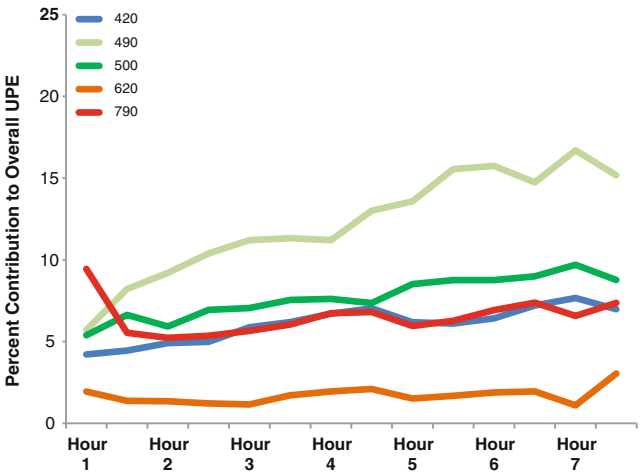

Fig. 8 Percent contribution of each of the visible wavelengths tested (420, 490, 500, 620, and 790 nm) to overall UPE as a function of time. Overall contribution was calculated by subtracting noise (dark counts) from the raw scores for each wavelength measured and dividing each wavelength's UPE by overall UPE (raw minus noise) from untreated cells with no filter. During the first 90 min, the combination for all seven responsive filters (sum=70 nm) contributed to 30 to 40 % of the total photon output

The most consistent quantitative change associated with effective facilitation of photon emission by molecular activators or diminishment by molecular inhibitors was the shift of more or less ~5 photon counts s^{-1} with respect to untreated baseline levels (~25 photon counts s^{-1}) for all treatments. The relatively fixed quantity of increased or decreased photon counts with activators and inhibitors, respectively, suggest a boundary condition. Whether this was related to the fixed concentration of the compounds, the fixed numbers of receptor molecules that mediate their effects on the cells' plasma membranes or to the restraints of intrinsic kinetics for these biomolecular reactions is not clear at this time.

The functional emission, when the directionality of the photons and the cross-sectional area are accommodated (a multiplication factor of about 40), was either an enhancement of 400 photons s^{-1} or diminishment of this amount within the population of ~$0.5 \cdot 10^6$ cells. Assuming that each photon is associated with an interaction with a structure within the plasma membrane, this would suggest that the activators and inhibitors were producing about 400 reactions/s for several hours of measurement.

The dosages of compounds contained within the cell media were $2.5\ 10^{-6}$ L $dish^{-1}$; $5\ 10^{-6}$ M L^{-1}; $6.023\ 10^{23}$ molecules M^{-1} or ~$7.5\ 10^{12}$ molecules of agent. Within 2.5 cm^3 ($2.5\ 10^{-6}$ m^3) of media containing the cells, this would be $0.3\ 10^{-18}$ m^3 per molecule or an effective length of 0.6 nm. Such density would be sufficient to occupy ion channels or to influence the distribution of the layer of charge that

contributes to the resting membrane potential (Persinger 2010). Our (Dotta et al. 2011a; Dotta et al. 2011b) previous experiments have implicated the equilibrium chemistry associated with the plasma membrane as the primary source of UPE in these cells.

One of the interesting quantitative anomalies was the discrepancy between the percentages of photons for all of the seven filters that contributed. Assuming equal distribution across the 580-nm band to which the PMT responded (370 to 950 nm), the summed increment of 70 nm should have contributed ~10 %. We measured about three to four times the numbers. We suggest one explanation that could also accommodate this discrepancy as well as the slow rise in photon emissions over time. The actual filter mechanism is based upon a series of mirror-like processes which results in the reflection of the nonfilter band photons back to the source. If photons are the primary stimuli that initiate the major changes in cell activity, including the metabolic and signaling processes associated with photon emissions, then this enhancement would be expected. This pattern could be interpreted as additional support for the quintessential role of very small quantities of photons within the visible and near-infrared and ultraviolet bands as the initiators of myriad molecular processes involved with cell proliferation, repair, and adaptation.

General significance

The concept of duality of matter and energy within biological systems has had a long history. Whereas the manifestations of matter are presented as spatial patterns (molecular structures), the manifestations of electromagnetic energy are presented as temporal patterns (frequency). The quantitative transformation or equivalence between matter and energy, although both contribute to cellular function, has been considered by some as spurious or even incomprehensible. The observation, centered on cells adapting to a shift from normal to abnormal conditions exhibiting a time-dependent shift in the wavelengths of the photons that are emitted, is consistent with the coupled relationship between molecular states of cell function and specific quantum of electromagnetic energies within the ultraviolet to near-infrared range. Cosic's rational molecular structures based upon a model that predicts optimal wavelengths of light from a representation of the distribution of free electron energy along a protein, that is, delocalized electrons of each amino acid that constitutes the protein, may contain the "Rosetta Stone" or code by which complex molecular structure and electromagnetic frequency can be equated. The experimental results, which prove compounds as activators or inhibitors based upon these predictions actually enhanced or diminished photon emissions, strongly support the theory's validity.

References

Bensaude O (2011) Inhibiting eukaryotic transcription. Transcription 2: 103–108

Bondos SE, Tan XX (2011) Combinatorial transcriptional regulation: the interaction of transcription factors and cell signaling molecules with homeodomain proteins in Drosophila development. Crit Rev Eukaryote Gene Expr 11:145–171

Chang JJ, Popp FA (1998) Biological organization: possible mechanism based on coherence of "biophotons". In: Chang JJ et al (eds) Biophotons. Kluwer Pub, Boston, pp 217–222

Choi DH, Lee KH, Moon JJ, Kim Y, Lim JH, Lee J (2012) Effect of 710 nm visible light irradiation on neurite outgrowth in primary rat cortical neurons following ischemic insult. Biochem Biophys Res Com 422:274–279

Cohen S, Popp FA (1997) Biophoton emission of the human body. J Photochem Photobiol B Biol 40:187–189

Cosic I (1994) Macromolecular bioactivity: is it resonant interaction between macromolecules? Theory and application. IEEE Trans BioMed Eng 41:1101–1114

de Souza SC, Munin E, Alves LP, Castillo Salgado MA, Pacheo MTT (2005) Low power laser radiation at 685 nm stimulates stem-cell proliferation rate in *Dugesia tigrina* during regeneration. J Photochem Photobiol B Biol 80:203–207

Dotta BT, Buckner CA, Cameron D, Lafrenie RM, Persinger MA (2011a) Biophoton emissions from cell cultures: biochemical evidence for the plasma membrane as the primary source. Gen Physiol Biophys 30:301–309

Dotta BT, Buckner CA, Lafrenie RM, Persinger MA (2011b) Photon emissions from human brain and cell culture exposed to distally rotating magnetic fields shared by separate light-stimulated brains and cells. Brain Res 388:77–88

Gossen M, Binin AL, Freundlieb S, Bujard H (1994) Inducible gene expression systems for higher eukaryotic cells. Curr Opin Biotechnol 5:516–520

Gurwitch AG (1923) Das problem der zellteilung physiologisch betrachtet. In: Gurwitsch AG et al. (eds) Monographien aus dem Gesamtgebiet der Physiologie der Pflanzen und der Tiere, pp 473–475

Isojima Y, Isoshima T, Nagai K, Kikuchi K, Nakagawa H (1995) Ultraweak biochemiluminescence detected from hippocampal slices. NeuroReport 6:658–660

Liu TC, Liu R, Zhu L, Yuan J, Hu M, Liu S (2009) Homeostatic photobiomodulation. Front Optoeletron China 2:1–8

Mitsunaga M, Ogawa M, Kosaka N, Rosenblum L, Choyke P, Kobayashi H (2011) Cancer cell-selective in vivo near infrared photoimmunotherapy targeting specific membrane molecules. Nat Med 17:1685–1691

Persinger MA (2010) 10^{-20} joules as a neuromolecular quantum in medicinal chemistry: an alternative approach to myriad molecular pathways? Cur Med Chem 17:3094–3098

Popp FA (1979) Photon storage in biological systems. In: Popp FA, Becker G, Konig HL, Pescha W (eds) Electromagnetic bioinformation. Urban and Schwarzenberg, Munich, pp 123–149

Popp FA (1988) Biophoton emission. Experientia 44:543–630

Sun Y, Wang C, Dai J (2010) Biophotons as neural communication signals demonstrated by in situ biophoton autography. Photochem Photobiol Sci 9:315–322

Tilbury RN, Quickenden TI (1988) Spectral and time dependence studies of the ultraweak bioluminescence emitted by the bacterium *Escherichia coli*. Photochem Photobiol 47:145–150

Wu HP, Persinger MA (2011) Increased mobility and stem-cell proliferation rate in *Dugesia tigrina* induced by 880 nm light emitting diode. J Photochem Photobiol B Biol 102:156–160